Direct and Reagentless Atmospheric Pressure Photoionisation Mass Spectrometry: Rapid and Accurate Differentiation of Cystic Fibrosis Related Bacteria by Monitoring VOCs

Adam Haworth-Duff
University of Liverpool
Barry L. Smith
University of Liverpool
Tung-Ting Sham
University of Liverpool
Cedric Boisdon
University of Liverpool
Paul Loughnane
University of Liverpool
Mark Burnley
University of Liverpool
Daniel B. Hawcutt
University of Liverpool
Rasmita Raval
University of Liverpool
Simon Maher
s.maher@liverpool.ac.uk

University of Liverpool

Article

Keywords:

Posted Date: February 27th, 2024

DOI: https://doi.org/10.21203/rs.3.rs-3976993/v1

Additional Declarations: No competing interests reported.

Abstract

Breath analysis is an area of significant interest in medical research as it allows for non-invasive sampling with exceptional potential for disease monitoring and diagnosis. Volatile organic compounds (VOCs) found in breath can offer critical insight into a person's lifestyle and/or disease/health state. To this end, the development of a rapid, sensitive, cost-effective and potentially portable method for the detection of key compounds in breath would mark a significant advancement. Herein we have designed, built and tested a novel reagent-less atmospheric pressure photoionisation (APPI) source, coupled with mass spectrometry (MS), utilising a bespoke bias electrode within a custom 3D printed sampling chamber for direct analysis of VOCs. Optimal APPI-MS conditions were identified including bias voltage, cone voltage and vaporisation temperature. Calibration curves were produced for ethanol, acetone, 2-butanone, ethyl acetate and eucalyptol, yielding $R^2 > 0.99$ and limits of detection < 10 pg. As a pre-clinical proof of concept, this method was applied to bacterial headspace samples of Escherichia coli (EC), Pseudomonas aeruginosa (PSA) and Staphylococcus aureus (SA) collected in 1 L Tedlar bags. In particular, PSA and SA are commonly associated with lung infection in cystic fibrosis patients. The headspace samples were classified using principal component analysis with 86.9% of the total variance across the first three components and yielding 100% classification in a blind-sample study. All experiments conducted with the novel APPI arrangement were carried out directly in real-time with low-resolution MS, which opens up exciting possibilities in the future for on-site (e.g., in the clinic) analysis with a portable system.

Introduction

Breath analysis is a significant and expanding area of medical research involving non-invasive sampling of continuously available, chemically rich bio-media.[1-3] Breath is primarily composed of O_2, N_2, CO_2, water vapour, volatile organic compounds (VOCs)[4,5] and non-volatile components[6,7]. Information pertaining to an individual's health status[8,9] can be acquired via monitoring disease biomarkers in exhaled breath[2,10]. A wide range of techniques are available for breath analysis, each focusing on distinct components of exhaled breath – certain methods target specific analytes, while others consider patterns of compounds, exhaled breath condensate, and gases, collectively offering complementary insight. By monitoring VOCs in breath it is possible to augment diagnosis and monitor specific diseases such as diabetes,[8,11,12] asthma[13-15] and lung disease.[16-18]

Cystic fibrosis (CF) is a debilitating genetic condition causing mucus hyper-concentration and decreased mucociliary clearance, leading to chronic lung infections.[19] Early diagnosis and rapid treatment of lung infections in CF patients is critical to decrease morbidity and extend life expectancy. Diagnosing infections from bacteria such as *Pseudomonas aeruginosa* (PSA) and *Staphylococcus aureus* (SA) can be problematic, particularly in infants since conventional tests are invasive.[20] For example, induced-sputum testing requires injecting saline solution into the nasal cavity of infants, an unpleasant experience for patients and frequently mis-administered. Bronchoscopy is highly effective for early

diagnosis but requires repeated anaesthesia for CF patients.[21] Less invasive tests lack sensitivity or reliability such as lung function measurements, cough swabs or cough plates. Imaging of lung tissue including chest x-rays is effective but is relatively expensive and exposes the patient to regular radiation doses.[22]

Analysing breath for diseases, such as CF, can significantly reduce the risk of new or chronic infections (from the same or secondary bacteria). Non-invasive methods of analysing bacterial presence may also help prevent unnecessary prescribing of antibiotics. It is therefore valuable to develop a method that is amenable for online breath analysis to enable detection of early-stage infection in CF patients. Ideally, any envisioned non-invasive diagnostic test should have requisite analytical performance whilst also being deployable at the point of care, with minimum risk of harm to patients. Mass spectrometry (MS) is especially suited to this task and in recent years several online or non-invasive MS-based assays have been reported.[23] A wide range of techniques are available for the analysis of VOCs in breath and bacterial headspaces, with methods targeting specific analytes or profiles of VOCs. The gold standard for VOC analysis is widely considered to be gas chromatography-mass spectrometry (GC-MS) for both qualitative and quantitative determination.[4,24] GC-MS has been applied to a wide range of headspace samples[12,25,26] and gaseous samples including breath.[12,27] Chromatographic techniques are powerful but inhibit on-line/ real-time analysis. For instance, GC-MS typically requires extensive sampling stages, such as solid-phase microextraction[27-30] or thermal desorption.[4] Extensive research efforts have been applied to secondary electrospray ionisation (SESI)[31], selected ion flow tube (SIFT)[32] and proton transfer reaction (PTR)[33] as these can offer on-line breath analysis.

Electrospray ionisation (ESI) and atmospheric pressure chemical ionisation (APCI) are amongst the most widely used ionisation techniques in molecular MS. In comparison to ESI and APCI, atmospheric pressure photoionisation (APPI) is relatively underutilised. Yet, APPI offers many advantageous qualities for VOC analysis. Ionisation of analyte molecules occurs if the ionisation energy (IE) of the analyte molecule is lower than the photon energy emitted from the UV lamp (10.6 eV being most common). APPI can ionise a broader range of compounds, in terms of molecular polarity, compared to ESI, and is less susceptible to matrix and ion suppression effects compared to APCI.[34,35] Furthermore, the inability of 10.6 eV lamps to ionise N_2, O_2 and CO_2 directly minimises background interferences aiding quantification and repeatability. The probability of an ionisation event occurring in APPI is, however, relatively low due to the mismatch in photon flux and the number of analyte molecules present. This is likely further reduced by the simultaneous generation of positive and negative ions that co-exist in the same volume and can lead to some fractional losses due to recombination events.

Photoionisation(PI)-based methods for breath analysis is a growing area of research[36]. Recently, Zhang *et al*[37] achieved good sensitivity detecting SARS-COV-2 infection using PI with high-resolution MS (HRMS) and machine learning (ML) based on breath VOC profiles. Zhou *et al*[38] modified a commercial APPI front end to facilitate breath sampling/analysis[38]; using a high-resolution Q-ToF and collision induced dissociation (CID) they reported identification of new metabolites in breath. As highlighted by

Drabińska *et al*[39], the presence or absence of individual VOCs as disease biomarkers can be misleading and often erroneously assigned. Taking a holistic approach in combination with chemometrics can be advantageous as ion combinations and metabolite fingerprints can be used to readily identify different bacteria. Hundreds of VOCs have been linked to different bacteria strains,[40-42] thus taking a holistic VOC fingerprinting approach is a viable option.[43-45]

In this study we demonstrate the effectiveness of a novel APPI-MS setup. This consists of a low-cost, 3D printed sample delivery system consisting of an APPI lamp, bias electrode, gas delivery ports and optional liquid dispensing vaporising heater. Traditionally for APPI analysis, a gaseous dopant molecule (often acetone or toluene) is added to the reagent gas stream in order to improve sensitivity and enhance detection limits.[46] Dopant ions facilitate charge transfer reactions to ions with greater proton affinity (PA) inducing ionisation in molecules that have higher IE than photons produced by the lamp[47]. Ionisation pathways in APPI broadly follow APCI patterns and have been extensively discussed in many review articles[47-49]. Herein we demonstrate the applicability of a reagent-less APPI method, that is easily accessible for online and direct analysis of VOCs. The method has been developed to enable real-time analysis. Moreover, development has been carried out using a low-resolution mass spectrometer (i.e., with performance metrics akin to a portable system). Following extensive method optimisation and characterisation, bacterial headspace is analysed, specifically SA and PSA cultures demonstrating excellent identification performance (100% classification; blind study of 6 samples), laying the foundation for future clinical investigations concerned with online breath analysis.

Results And Discussion

APPI-MS Interface and Novel Bias Electrode Characterisation

Figure 1 shows a cross-section of the inner structure of the APPI interface. The UV lamp (8) and driver electronics were harnessed from a commercial APPI source (ThermoFisher). The grounded metal collar (7) surrounding the lamp (8) forms a gas tight seal with a bespoke 3D printed enclosure (6). A photopolymer resin material was used rather than the more common extruded (fused deposition) plastic type due to better outgassing characteristics of UV-cured resin when under UV irradiation (from the APPI lamp). The lamp is inserted such that the front face of the lamp aligns with the back edge of the 3D printed chamber. Here a thin (0.4 mm) metal electrode (4) is located to apply a positive potential bias, with respect to the inlet (1), to confer positive ions created in the ionisation chamber a drift velocity in the direction of the MS inlet. PTFE spacers (10) with holes drilled to enable gas entry and exit provide an ionisation volume directly in front of the MS inlet. A second thin electrode (3) provides the reference potential for the bias voltage and is electrically connected to the sampling cone of the mass spectrometer. Finally, a 3D printed piece (2) push-fits over the sampling cone, and threaded rods/nuts compress each element into a gas tight sampling chamber. It should be noted that the final 3D printed piece can be readily designed to fit onto any mass spectrometer atmospheric pressure interface (API) by changing the diameter of the exit orifice to suit. Rubber bungs with stainless steel and PTFE hoses

provide gas entry (5) and exit (9) from the source via either pressurisation from the inlet region or evacuation by a small diaphragm pump at the exit.

An offline characterisation of the ion distribution generated by the UV lamp was performed to aid design of the APPI-MS interface. Figure 2 depicts the resultant application of a potential bias between UV lamp and segmented detector. A steady and substantial increase in total measured ion current (cumulative ion current hitting individual strips) as electric field intensity is increased from 0 V/mm to approximately 50 V/mm is observed, which subsequently plateaus for higher field strengths. The increasing force and therefore ion velocity due to the increase in applied field yields an order magnitude increase in ion transmission to the detector. This is likely, at least in part, due to limiting recombination processes between positive and negative ions in the irradiance chamber. Plotting the ion current measured on individual strips enables visualisation of the ion beam cross-sectional area. Figure 2 insert shows the ion distribution; the ion current is plotted for each strip with the applied voltage between the bias electrode and detector set at 1000 V, corresponding to an electric field intensity of 50 V/mm. The irradiance diameter at maximum ion transmission was approximately 14 mm, decreasing from 35 mm under no potential bias conditions. The diameter of the internal irradiance chamber was therefore constructed to be 20 mm to avoid charging of the insulating 3D printed plastic. Some surface charging of the internal wall structure is expected and we expect this will act to further confine the ion cloud diffusion[50], thereby increasing the quantity of ions sampled by the MS inlet. Furthermore, utilising the smallest irradiance volume possible also reduces neutral analyte diffusion, thereby potentially improving ionisation efficiency due to increased analyte concentration.

Parameter Optimisation

To establish the optimal operating conditions, a series of experiments were performed to assess each of the tuneable parameters in the design for a range of compounds related to breath analysis. Ethanol, acetone, ethyl acetate, 2-butanone and eucalyptol were examined. These compounds were selected to encompass a range of breath related VOCs, with a mass range from 47 to 155 amu and boiling points ranging from 56°C to 176°C.

Cone Bias Voltage

Cone voltage and potential bias electrode are coupled parameters therefore they were optimised in tandem; Figure 3 shows the signal intensity heatmaps for each compound examined. Supplementary Figure S2 shows the average mass spectrum extracted from the maximised bias and cone voltage experiments for each analyte. Applying potential bias between lamp and inlet improves the signal intensity by a factor of ~10 for all analytes examined. Maximised signal intensity occurs at a bias voltage of 200 V for each compound. It would be of interest to examine higher mass analytes to establish if a broad mass dependency exists but this is out of scope for purposes of this present study. Water (m/z 37) and ethanol (m/z 47) both yielded a narrow band of cone voltages that gave relatively high signal intensities from 10 V to 20 V and 15 V to 25 V, respectively. Outside of these narrow ranges the signal

intensity dropped off significantly. Acetone and 2-butanone also shared a signal intensity response but instead of bands, in the heat map depiction, they formed concentric circles of increasing signal intensity, peaking at 200 V and 35 V and 200 V and 30 V for bias and cone voltages, respectively. Acetone and 2-butanone showed a higher degree of tolerance towards unoptimised conditions than water or ethanol. Ethyl acetate and eucalyptol exhibited similar concentric circular profiles to acetone and 2-butanone but with a smaller tolerance for unoptimised parameters. Optimum values for bias and cone voltages for ethyl acetate and eucalyptol were both 200 V and 20 V, respectively. Thus, for the remainder of the study, a 200 V bias voltage and 20 V cone voltage were selected to give broadly optimal transmission (~10-fold increase compared to no bias electrode) over the mass range of interest.

Carrier Gas Flow Rates

Introduction of standards into the APPI chamber is conducted via dosing liquid analytes into an N_2 carrier gas at precise flow rates using a syringe pump driver (SS Scientific). A 1/16” stainless steel capillary is concentrically inserted into a ¼” stainless steel tube and fixed using Swagelok compression fittings. The flow rate of the carrier gas is adjustable via a mechanical variable area flow meter (Brooks Instruments) within the range 0-5 $Lmin^{-1}$. The liquid solution is dispensed to the end of the capillary where subsequent nebulisation and transportation to the APPI lamp is facilitated via the carrier gas. A tubular heating element is placed outside of the ¼” tubing to aid vaporisation of the analyte. No significant carryover is observed when the syringe driver is stopped; after a few seconds the analyte signal returns to background level.

A series of experiments were performed to determine the response of the system to sample and gas flow rate changes for a 20 ppm solution of eucalyptol in water. Figure 4 shows the signal intensity of the $[M+H]^+$ protonated molecular ion for eucalyptol for each gas flow rate tested. The amount of eucalyptol introduced into the carrier gas stream was 0.5, 1, 2, 5 and 10 $\mu Lmin^{-1}$ corresponding to 15.4, 30.7 61.4 153.5 and 307.0 pg of analyte. The nitrogen gas flow rate was varied between 1 and 5 $Lmin^{-1}$ in 1 $Lmin^{-1}$ steps. For carrier gas flow rates above 3 $Lmin^{-1}$, the signal response was linear across the range investigated (R^2 = 0.996, 0.998 and 0.995 for 3, 4 and 5 $Lmin^{-1}$, respectively). For 1 and 2 $Lmin^{-1}$, a reduced upper limit of linearity was observed. The loss in dynamic range is attributed to the higher concentration of water vapour in the gas stream. It is well known that increased solvent concentration supresses analyte signal in APPI due to absorption of photons by the much higher concentration of solvent[51,52]. The choice of water here was intended to gauge the applicability of the system for future breath analysis which contains a relatively high moisture content. Increased signal response for lower carrier gas flow rates is due to a reduced dilution of the analyte in the carrier gas stream. A carrier gas flow rate of 5 $Lmin^{-1}$ was used to produce calibration curves, whilst bacteria headspace sampling was carried out using a reduced carrier gas flow rate of 0.2 $Lmin^{-1}$ to improve sensitivity.

Vaporisation Temperature

The final element investigated to determine optimal operation was the vaporising heater temperature. A series of experiments were performed by increasing the vaporising heater temperature from 30 °C to 190 °C in 20 °C steps. 20 ppm solutions of acetone, 2-butanone and eucalyptol in water were individually prepared for optimisation. Each analyte was fed into the capillary and the temperature allowed to stabilise before a measurement was initiated. Figure 5 (a) shows the signal intensity of *m/z* 59, 73 and 155 peaks relating to acetone, 2-butanone and eucalyptol, respectively, for each temperature set. The intensity values generally increase with increasing temperature for all analytes. Presumably this is due to more efficient vaporisation of the analyte which reduces any condensation losses onto the hoses and/or chamber structure. In the case of eucalyptol this increase was continuous as temperature increased, however acetone (b.p. 55.8°C) and 2-butanone (b.p. 79.5°C) peaked at ~130 °C and ~150 °C, respectively, before declining, possibly due to thermal degradation of these analytes. Eucalyptol has the highest boiling point of the three analytes assessed. Whilst increasing the temperature appears advantageous in terms of individual analyte sensitivity, Figure 5 (b) depicts the relative height of the peaks in respect to the total ion current. It can be observed that increasing the temperature reduces the signal-to-noise ratio of the peaks of interest, possibly due to the other system contaminants being thermally desorbed from the APPI chamber material and gas delivery system. Since the goal of the present study is to determine the metabolite profile of different bacterial samples, the temperature was fixed at 70 °C to avoid the emergence of spurious peaks at the expense of sacrificing some sensitivity.

Quantification and Limits of Detection

Calibration curves were produced for each compound diluted in ultra-pure water. Individually, each analyte (ethanol, acetone, 2-butanone, ethyl acetate and eucalyptol) produced a highly linear calibration curve with a coefficient of determination ≥ 0.99 (supplementary information, Table S1). The calibration curves can be found in supplementary information Figure S2; ethanol produced a linear response between 31 ppbv and 315 ppbv, acetone and 2-butanone gave linear responses between 2 ppbv and 25 ppbv, ethyl acetate and eucalyptol also gave linear responses between 3 ppbv and 36 ppbv.

Ethanol can be found in breath due to bacterial activity in the gut[53,54] with expected concentrations in healthy breath between 10-1000 ppb. Ethanol's presence can also give information about lifestyle such as recent consumption of alcohol. Acetone is another VOC naturally found in breath at approximately 1-1000 ppbv[54] with elevated concentrations greater than 1800 ppbv corresponding to patients with diabetes mellitus.[11,12] In isolation acetone detection is permissible with a limit of detection (LOD) of 6.8 ppbv and limit of quantification (LOQ) of 27.8 ppbv. The APPI-MS method is also suitable for the detection of 2-butanone with an LOD of 1.6 ppbv and LOQ of 6.5 ppbv, which is normally present in the breath of healthy people at approximately 20 ppbv[5,55] and is found in the headspace of bacteria samples of *Pseudomonas aeruginosa*.[41] Some have suggested ethyl acetate is a potential marker related to lung disease.[56] When analysing the breath of these patients, ethyl acetate may be present in concentrations up to 100 ppb[5] which is undetectable in the breath of a healthy person. Our method is suitable for ethyl acetate analysis with an LOD of 0.7 ppbv and an LOQ of 5.0 ppbv. Finally, eucalyptol was detectable at

0.9 ppbv and quantifiable at 4.8 ppbv. Eucalyptol was included for future reference, as it is not expected to be found in breath naturally, but can be found if an individual has recently consumed mint.

Bacterial Culture Classification

To assess the suitability of the apparatus for potentially determining the bacterial origin of lung infections in CF patients, PSA and SA cultures were prepared and sampled using 1 L Tedlar bags as described in the methods section. A further cautionary note on Tedlar bag suitability for direct analysis, such as ambient ionisation techniques, can be found in supplementary information. The resultant collected headspace was evacuated from the bag and passed through the APPI chamber by pumping via a small diaphragm pump. Samples were collected and analysed in batches of four over a three-week period. A new culture was initiated each Monday and samples collected on the subsequent Friday, in total 12 of each type of bacterial headspace was sampled. *Escherichia coli* (EC) which is unrelated to CF was included as a control and as a means to improve the robustness of the classification. Figure 6 shows centroided spectra for one PSA sample and one SA sample; only peaks with relative intensities above 20% were retained for display purposes. Immediately obvious are a number of distinct visual differences between samples with a significant number of peaks appearing in only one of the samples. This gives confidence that a classification model can successfully be applied to the dataset. The total ion chromatograms and time indexes of extracted spectra for all samples are shown in supplementary Figures S3-5.

After pre-processing spectral data as outlined in the methods section, 247 peaks were found across all samples and included in a principal component analysis (PCA) model. A data table containing 247 dependant variables and 36 observations was collated. PCA was compiled to visualise spectral differences and dimensionally reduce the dataset. The first three principal components accounted for 86.9 % of the total variance which is an excellent result. A PCA biplot can be seen in Figure 7 displaying excellent separation and grouping of sample classes with clear class boundaries evident for all 3 groups. Principal component (PC)1 is the discriminating component for EC and PSA whilst PC2 was responsible for separation of SA. The remaining PCs (not shown) were not found to differentiate between the sample classes.

Following PCA, a linear discriminant classification model was built using the 247 features. 10 times cross validation was used to avoid overfitting and improve robustness. 100% of samples were correctly classified by the model. This was a very pleasing and significant result, since the samples included multiple cultures, with sample collection compiled and analysed over several weeks. A further set of three SA and three PSA headspace samples was acquired a week later from a fresh batch of cultures. Class predictions were made by the model generated from the training data set in a blind study. 100% of the blind study samples were correctly classified. The results are comparable to that of current SESI-MS and SIFT-MS methods.[40,43] The confusion matrix showing classification results is shown in supplementary Figure S6. Since our laboratory is not designated to handle Class 2 bacterial cultures, it was not possible to conduct online sampling/analysis. Therefore, non-ideal Tedlar bag sampling was used to collect the

headspace (Figures S7 & S8). Presumably even better results could have been achieved with direct headspace sampling. Nevertheless, a low-resolution mass spectrometer and without requiring tandem mass analysis, this approach has correctly identified SA and PSA in real-time and directly from gaseous samples, without the need of reagents, such as dopants previously identified in APPI studies or reagents for SESI. This shows the excellent potential of this approach to be extended for online breath analysis in-clinic with a portable system; for example, to aid diagnosis or to monitor treatment effectiveness.

Conclusions

In this study a novel APPI-MS approach has been designed to facilitate non-invasive, real-time and direct breath sampling for detection of bacterial infection in CF patients, with preliminary experiments examining bacterial headspace as a proxy for this case. A thorough investigation and characterisation of the new sampling apparatus and methodology has been carried out. We conducted extensive optimisations using a range of compounds that are relevant to breath analysis, establishing limits of detection and quantification in concentration ranges that are of medical interest. The analysis is carried out directly on the headspace in real-time using reagent-less APPI. Finally, a classification study was conducted using bacterial headspace from PSA and SA cultures (which also included EC), two prominent sources of bacterial infection in CF patients. Excellent separation and grouping were achieved in PCA space, with 100% classification accuracy for a small blind study (of 6 samples), using a low-resolution mass spectrometer in full MS mode (i.e., without requiring tandem capability). This is a significant result, as it demonstrates the possibility of carrying out breath analysis in-clinic with a portable (low-resolution) mass spectrometer, which is the subject of future work.

Methods

MS Settings

All experiments were performed on a Waters Xevo triple quadrupole mass spectrometer (TQ-MS); a low-resolution mass spectrometer (mass resolution ~ 0.4 amu, FWHM) released in 2007. As our long-term goal is to develop a method suitable for real-time in-clinic breath analysis, it is necessary to develop our approach on a mass spectrometer with similar performance to a portable mass spectrometer.

Full scan mode was used with a mass acceptance window of 20 to 300 amu and the scan acquisition time was set to 2 seconds per scan unless otherwise stated. APPI is an ambient ionisation method.[57–62] Modifications were made to the instrument front-end to make efficient use of the available hardware and to minimise the peripheral equipment needed to operate the bespoke APPI chamber. Tapped threads were drilled into the gas entry ports usually supplying N_2 gas to the commercial ESI source. Push fit pneumatic connectors were inserted into the threaded taps to connect a variable area flow meter whereby the user can manually set a carrier gas flow rate. N_2 was supplied by a nitrogen generator (Peak Scientific). A custom cable (LEMO) was constructed to connect the bias electrode to the HV power supply available on the front of the instrument. This enables software selection of the bias potential via the MS tune page in

MassLynx. Finally, the interlock to prevent operation without the ESI front end in place was overcome though fixing a small metal pin to depress the microswitch. Apart from the stated modifications and unless otherwise stated, the instrument was operated as per the manufacturer's recommendations.

Chemicals and Reagents

A range of chemicals were purchased for analysis including: ethanol (GC standard grade), acetone (> 99.8% HPLC grade), ethyl acetate (99.7% HPLC grade) and eucalyptol (99%) purchased from Sigma Aldrich, and 2-butanone (> = 99%) from VWR. The VOC standards were diluted in ultra-pure water (v/v) from a Direct-Q 3UV ultra-pure (type 1) water system (18.2 MΩ).

Source Characterisation

An offline measurement of the ion distribution generated from the UV lamp was performed, supplementary Figure S1 depicts the experimental configuration. A stainless-steel electrode was fixed 20 mm from a segmented Faraday plate detector (designed and built in-house)[63]. The sensor contains fifty, 0.85 mm wide x 15 mm length, sensing elements capable of simultaneously integrating the ion current striking each strip of the detector. A 12 mm diameter opening was cut into the bias electrode to enable the UV lamp insertion. A voltage applied to the biasing electrode was scanned between 0 V and 2000 V in 100 V steps. After each new applied voltage, the ion current hitting each of the 50 strips on the detector was measured and recorded.

Bacteria Sampling

The bacteria were initially grown on agar gel, in which 1 mL of the culture was transferred to 200 mL of LB broth (MILLER) purchased from Merck, in a 1 L conical flask with a gauze bung and left on a shaker bed at 220 rpm in a temperature controlled dark room (37°C). The bacteria were incubated overnight. After incubation, bacterial headspaces were actively sampled by placing stainless steel tubing into the conical flask and removing gas phase constituents via a peristaltic pump with verderprene tubing for 2 minutes at a rate of approximately 400 mL/min. 1 L Tedlar bags were used for collection and transferred to the mass spectrometry laboratory for analysis within 1 hour after sampling. All bacteria analyses were conducted over a 3-week period in total.

After collection, each sample was evacuated with the APPI-MS interface using a pump set at 400 mL/min over a time period of 5-minutes. At the same time, corresponding data files were generated on the mass spectrometer and processed accordingly to yield average spectra for each sample.

Data Processing

Raw data collected from each sample was stored in separate MassLynx files; these were named based on method parameters, sample and repeat information. Conversion from MassLynx .RAW to .mzXML was completed prior to data processing and analysis undertaken in MATLAB R2022b (Mathworks). A series of pre-processing steps is performed on the dataset prior to use in classification models.[64,65] Briefly, after mzXML files are extracted into a MATLAB data table, the retention times and total ion currents (TIC) are

extracted and searched for abrupt changes in TIC current, indicating the beginning and end of sampling the contents of a Tedlar bag. 5 scans were removed at the beginning and end for every sample to discount any variation during the transient periods. The scans between the two time indexes generated by the MATLAB function findchangepoints() were averaged into a single scan. The intensity information is smoothed and resampled over a uniform 0.1 u grid and normalised. MATLAB function findpeaks() is used to extract the peak height information and the peak location. To avoid multiple peaks sampled with small m/z shifts affecting classification, the location of each peak was rounded to the nearest integer. The peak information was located into a single table and any missing peaks not generated by the find peaks algorithm across samples were assigned the value 0. Furthermore, a threshold of 0.5% was applied to the data with any peaks below the threshold assigned a 0 value.

References

1. Berchtold, C., Bosilkovska, M., Daali, Y., Walder, B. & Zenobi, R. Real-time monitoring of exhaled drugs by mass spectrometry. Mass Spectrom Rev 33, 394–413, doi:10.1002/mas.21393 (2014).
2. Pleil, J. D., Stiegel, M. A. & Risby, T. H. Clinical breath analysis: discriminating between human endogenous compounds and exogenous (environmental) chemical confounders. Journal of Breath Research 7, 017107, doi:10.1088/1752-7155/7/1/017107 (2013).
3. Rattray, N. J., Hamrang, Z., Trivedi, D. K., Goodacre, R. & Fowler, S. J. Taking your breath away: metabolomics breathes life in to personalized medicine. Trends Biotechnol 32, 538–548, doi:10.1016/j.tibtech.2014.08.003 (2014).
4. Lawal, O., Ahmed, W. M., Nijsen, T. M. E., Goodacre, R. & Fowler, S. J. Exhaled breath analysis: a review of 'breath-taking' methods for off-line analysis. Metabolomics 13, 110, doi:10.1007/s11306-017-1241-8 (2017).
5. Fenske, J. D. & Paulson, S. E. Human breath emissions of VOCs. J Air Waste Manag Assoc 49, 594–598, doi:10.1080/10473289.1999.10463831 (1999).
6. Syslova, K. *et al.* Determination of cysteinyl leukotrienes in exhaled breath condensate: method combining immunoseparation with LC-ESI-MS/MS. J Chromatogr B Analyt Technol Biomed Life Sci 879, 2220–2228, doi:10.1016/j.jchromb.2011.06.004 (2011).
7. Martinez-Lozano, P. & Fernandez de la Mora, J. Direct analysis of fatty acid vapors in breath by electrospray ionization and atmospheric pressure ionization-mass spectrometry. Anal Chem 80, 8210–8215, doi:10.1021/ac801185e (2008).
8. Manolis, A. The diagnostic potential of breath analysis. Clin Chem 29, 5–15 (1983).
9. Amann, A. *et al.* Applications of breath gas analysis in medicine. International Journal of Mass Spectrometry 239, 227–233, doi:https://doi.org/10.1016/j.ijms.2004.08.010 (2004).
10. Kim, K. H., Jahan, S. A. & Kabir, E. A review of breath analysis for diagnosis of human health. TrAC Trends in Analytical Chemistry 33, 1–8, doi:https://doi.org/10.1016/j.trac.2011.09.013 (2012).

11. Righettoni, M. *et al.* Breath acetone monitoring by portable Si:WO3 gas sensors. Anal Chim Acta 738, 69–75, doi:10.1016/j.aca.2012.06.002 (2012).
12. Deng, C., Zhang, J., Yu, X., Zhang, W. & Zhang, X. Determination of acetone in human breath by gas chromatography-mass spectrometry and solid-phase microextraction with on-fiber derivatization. J Chromatogr B Analyt Technol Biomed Life Sci 810, 269–275, doi:10.1016/j.jchromb.2004.08.013 (2004).
13. Deykin, A., Massaro, A. F., Drazen, J. M. & Israel, E. Exhaled nitric oxide as a diagnostic test for asthma: online versus offline techniques and effect of flow rate. Am J Respir Crit Care Med 165, 1597–1601, doi:10.1164/rccm.2201081 (2002).
14. Reynolds, J. C. *et al.* Analysis of human breath samples using a modified thermal desorption: gas chromatography electrospray ionization interface. J Breath Res 8, 037105, doi:10.1088/1752-7155/8/3/037105 (2014).
15. Takao, A., Shimoda, T., Kohno, S., Asai, S. & Harda, S. Correlation between alcohol-induced asthma and acetaldehyde dehydrogenase-2 genotype. J Allergy Clin Immunol 101, 576–580, doi:10.1016/S0091-6749(98)70162-9 (1998).
16. Dent, A. G., Sutedja, T. G. & Zimmerman, P. V. Exhaled breath analysis for lung cancer. J Thorac Dis 5 Suppl 5, S540–550, doi:10.3978/j.issn.2072-1439.2013.08.44 (2013).
17. Chan, H. P., Lewis, C. & Thomas, P. S. Exhaled breath analysis: novel approach for early detection of lung cancer. Lung Cancer 63, 164–168, doi:10.1016/j.lungcan.2008.05.020 (2009).
18. Santos, P. M., Del Nogal Sanchez, M., Pozas, A. P. C., Pavon, J. L. P. & Cordero, B. M. Determination of ketones and ethyl acetate-a preliminary study for the discrimination of patients with lung cancer. Anal Bioanal Chem 409, 5689–5696, doi:10.1007/s00216-017-0508-2 (2017).
19. Smyth, A. R. *et al.* European Cystic Fibrosis Society Standards of Care: Best Practice guidelines. J Cyst Fibros 13 Suppl 1, S23–42, doi:10.1016/j.jcf.2014.03.010 (2014).
20. Scott-Thomas, A. J. *et al.* 2-Aminoacetophenone as a potential breath biomarker for Pseudomonas aeruginosa in the cystic fibrosis lung. BMC Pulm Med 10, 56, doi:10.1186/1471-2466-10-56 (2010).
21. Kos, R. *et al.* Targeted exhaled breath analysis for detection of Pseudomonas aeruginosa in cystic fibrosis patients. J Cyst Fibros 21, e28-e34, doi:10.1016/j.jcf.2021.04.015 (2022).
22. Neerincx, A. H. *et al.* Detection of Staphylococcus aureus in cystic fibrosis patients using breath VOC profiles. J Breath Res 10, 046014, doi:10.1088/1752-7155/10/4/046014 (2016).
23. Maher, S., Jjunju, F. P. & Taylor, S. Colloquium: 100 years of mass spectrometry: Perspectives and future trends. Reviews of Modern Physics 87, 113 (2015).
24. Wang, X. R., Cassells, J. & Berna, A. Z. Stability control for breath analysis using GC-MS. J Chromatogr B Analyt Technol Biomed Life Sci 1097–1098, 27–34, doi:10.1016/j.jchromb.2018.08.024 (2018).
25. Cervera, M. I., Beltran, J., Lopez, F. J. & Hernandez, F. Determination of volatile organic compounds in water by headspace solid-phase microextraction gas chromatography coupled to tandem mass

spectrometry with triple quadrupole analyzer. Anal Chim Acta 704, 87–97, doi:10.1016/j.aca.2011.08.012 (2011).

26. Barhdadi, S. *et al.* Development and validation of a HS/GC-MS method for the simultaneous analysis of diacetyl and acetylpropionyl in electronic cigarette refills. J Pharm Biomed Anal 142, 218–224, doi:10.1016/j.jpba.2017.04.050 (2017).
27. Bouza, M., Gonzalez-Soto, J., Pereiro, R., de Vicente, J. C. & Sanz-Medel, A. Exhaled breath and oral cavity VOCs as potential biomarkers in oral cancer patients. J Breath Res 11, 016015, doi:10.1088/1752-7163/aa5e76 (2017).
28. Yuan, Z. C. *et al.* Solid-Phase Microextraction Fiber in Face Mask for in Vivo Sampling and Direct Mass Spectrometry Analysis of Exhaled Breath Aerosol. Anal Chem 92, 11543–11547, doi:10.1021/acs.analchem.0c02118 (2020).
29. Song, G. *et al.* Quantitative breath analysis of volatile organic compounds of lung cancer patients. Lung Cancer 67, 227–231, doi:10.1016/j.lungcan.2009.03.029 (2010).
30. Bristow, R. L. *et al.* An automated micro solid phase extraction gas chromatography–mass spectrometry (μSPE-GC–MS) detection method for geosmin and 2-methylisoborneol in drinking water. Scientific Reports 13, 1768, doi:10.1038/s41598-023-28543-x (2023).
31. Weber, R. *et al.* Volatile organic compound breath signatures of children with cystic fibrosis by real-time SESI-HRMS. ERJ Open Res 6, doi:10.1183/23120541.00171-2019 (2020).
32. Markar, S. R. *et al.* Breath Volatile Organic Compound Profiling of Colorectal Cancer Using Selected Ion Flow-tube Mass Spectrometry. Annals of Surgery 269 (2019).
33. Trefz, P. *et al.* Continuous Real Time Breath Gas Monitoring in the Clinical Environment by Proton-Transfer-Reaction-Time-of-Flight-Mass Spectrometry. Analytical Chemistry 85, 10321–10329, doi:10.1021/ac402298v (2013).
34. Dang, M., Liu, R., Dong, F., Liu, B. & Hou, K. Vacuum ultraviolet photoionization on-line mass spectrometry: Instrumentation developments and applications. TrAC Trends in Analytical Chemistry 149, 116542, doi:https://doi.org/10.1016/j.trac.2022.116542 (2022).
35. Jorabchi, K., Hanold, K. & Syage, J. Ambient analysis by thermal desorption atmospheric pressure photoionization. Anal Bioanal Chem 405, 7011–7018, doi:10.1007/s00216-012-6536-z (2013).
36. Wang, Y. *et al.* High-Pressure Photon Ionization Source for TOFMS and Its Application for Online Breath Analysis. Analytical Chemistry 88, 9047–9055, doi:10.1021/acs.analchem.6b01707 (2016).
37. Zhang, P. *et al.* A feasibility study of Covid-19 detection using breath analysis by high-pressure photon ionization time-of-flight mass spectrometry. Journal of Breath Research 16, 046009, doi:10.1088/1752-7163/ac8ea1 (2022).
38. Zhou, W. *et al.* Modification of an atmospheric pressure photoionization source for online analysis of exhaled breath coupled with quadrupole time-of-flight mass spectrometry. Analytical and Bioanalytical Chemistry 412, 3663–3671, doi:10.1007/s00216-020-02602-y (2020).
39. Drabińska, N. *et al.* A literature survey of all volatiles from healthy human breath and bodily fluids: the human volatilome. Journal of Breath Research 15, 034001, doi:10.1088/1752-7163/abf1d0

(2021).

40. Dryahina, K., Sovova, K., Nemec, A. & Spanel, P. Differentiation of pulmonary bacterial pathogens in cystic fibrosis by volatile metabolites emitted by their in vitro cultures: Pseudomonas aeruginosa, Staphylococcus aureus, Stenotrophomonas maltophilia and the Burkholderia cepacia complex. J Breath Res 10, 037102, doi:10.1088/1752-7155/10/3/037102 (2016).
41. Boots, A. W. *et al.* Identification of microorganisms based on headspace analysis of volatile organic compounds by gas chromatography-mass spectrometry. J Breath Res 8, 027106, doi:10.1088/1752-7155/8/2/027106 (2014).
42. Filipiak, W. *et al.* Volatile Organic Compounds (VOCs) Released by Pathogenic Microorganisms in vitro: Potential Breath Biomarkers for Early-Stage Diagnosis of Disease. Volatile Biomarkers, 463–512, doi:10.1016/B978-0-44-462613-4.00023-4 (2013).
43. Kaeslin, J. *et al.* Differentiation of Cystic Fibrosis-Related Pathogens by Volatile Organic Compound Analysis with Secondary Electrospray Ionization Mass Spectrometry. *Metabolites* 11, doi:10.3390/metabo11110773 (2021).
44. Drees, C. *et al.* GC-IMS headspace analyses allow early recognition of bacterial growth and rapid pathogen differentiation in standard blood cultures. Appl Microbiol Biotechnol 103, 9091–9101, doi:10.1007/s00253-019-10181-x (2019).
45. Bregy, L. *et al.* Differentiation of oral bacteria in in vitro cultures and human saliva by secondary electrospray ionization - mass spectrometry. Sci Rep 5, 15163, doi:10.1038/srep15163 (2015).
46. Bookmeyer, C., Soltwisch, J., Rohling, U. & Dreisewerd, K. Low-Pressure Photoionization in a Dual-Ion Funnel Injector Coupled to an Orbitrap Mass Spectrometer for Direct Analysis of Human Breath and Head-Space Sampled Coffee Roasts. Chempluschem 85, 1559–1563, doi:10.1002/cplu.202000462 (2020).
47. Raffaelli, A. & Saba, A. Atmospheric pressure photoionization mass spectrometry. Mass Spectrometry Reviews 22, 318–331, doi:https://doi.org/10.1002/mas.10060 (2003).
48. Robb, D. B. & Blades, M. W. State-of-the-art in atmospheric pressure photoionization for LC/MS. Analytica Chimica Acta 627, 34–49, doi:https://doi.org/10.1016/j.aca.2008.05.077 (2008).
49. Kauppila, T. J., Syage, J. A. & Benter, T. Recent developments in atmospheric pressure photoionization-mass spectrometry. Mass Spectrometry Reviews 36, 423–449, doi:https://doi.org/10.1002/mas.21477 (2017).
50. Iyer, K. *et al.* Ion Manipulation in Open Air Using 3D-Printed Electrodes. Journal of the American Society for Mass Spectrometry 30, 2584–2593, doi:10.1007/s13361-019-02307-2 (2019).
51. Kauppila, T. J., Bruins, A. P. & Kostiainen, R. Effect of the Solvent Flow Rate on the Ionization Efficiency in Atmospheric Pressure Photoionization-Mass Spectrometry. Journal of the American Society for Mass Spectrometry 16, 1399–1407, doi:https://doi.org/10.1016/j.jasms.2005.03.051 (2005).
52. Staff, R. A. E. S. H. *The PID Handbook: Theory and Applications of Direct-Reading Photoionization Detectors*. (RAE Systems by Honeywell, 2014).

53. Di Natale, C., Paolesse, R., Martinelli, E. & Capuano, R. Solid-state gas sensors for breath analysis: a review. Anal Chim Acta 824, 1–17, doi:10.1016/j.aca.2014.03.014 (2014).
54. Diskin, A. M., Spanel, P. & Smith, D. Time variation of ammonia, acetone, isoprene and ethanol in breath: a quantitative SIFT-MS study over 30 days. Physiol Meas 24, 107–119, doi:10.1088/0967-3334/24/1/308 (2003).
55. Van den Velde, S., Nevens, F., Van Hee, P., van Steenberghe, D. & Quirynen, M. GC-MS analysis of breath odor compounds in liver patients. J Chromatogr B Analyt Technol Biomed Life Sci 875, 344–348, doi:10.1016/j.jchromb.2008.08.031 (2008).
56. Khatoon, Z. *et al.* Ethyl Acetate Chemical Sensor as Lung Cancer Biomarker Detection Based on Doped Nano-SnO Synthesized by Sol-Gel Process. IEEE Sensors Journal 20, 12504–12511, doi:10.1109/JSEN.2020.3001285 (2020).
57. Zhou, Y. *et al.* Emergency diagnosis made easy: matrix removal and analyte enrichment from raw saliva using paper-arrow mass spectrometry. Analyst 148, 5366–5379, doi:10.1039/D3AN00850A (2023).
58. Sham, T.-T., Badu-Tawiah, A. K., McWilliam, S. J. & Maher, S. Assessment of creatinine concentration in whole blood spheroids using paper spray ionization–tandem mass spectrometry. Scientific Reports 12, 14308, doi:10.1038/s41598-022-18365-8 (2022).
59. Smith, B. L. *et al.* Ambient ion focusing for paper spray ionisation. Int. J. Mass spectrom. 471, 116737, doi:https://doi.org/10.1016/j.ijms.2021.116737 (2022).
60. Sarih, N. M. *et al.* Accelerated nucleophilic substitution reactions of dansyl chloride with aniline under ambient conditions via dual-tip reactive paper spray. Scientific Reports 10, 21504, doi:10.1038/s41598-020-78133-4 (2020).
61. Jjunju, F. P. M. *et al.* Analysis of non-conjugated steroids in water using paper spray mass spectrometry. Scientific Reports 10, 10698, doi:10.1038/s41598-020-67484-7 (2020).
62. Maher, S. *et al.* Direct Analysis and Quantification of Metaldehyde in Water using Reactive Paper Spray Mass Spectrometry. Scientific Reports 6, 35643, doi:10.1038/srep35643 (2016).
63. Smith, B. L. *et al.* in *2017 IEEE SENSORS.* 1–3.
64. Smith, B. L. *et al.* Rapid Scotch Whisky Analysis and Authentication using Desorption Atmospheric Pressure Chemical Ionisation Mass Spectrometry. Scientific Reports 9, 7994, doi:10.1038/s41598-019-44456-0 (2019).
65. Charoensumran, P. *et al.* Rapid geographical indication of peppercorn seeds using corona discharge mass spectrometry. Scientific Reports 11, 16089, doi:10.1038/s41598-021-95462-0 (2021).

Declarations

Acknowledgments

We would like to express our gratitude for the excellent support received from the electrical and mechanical workshops in the EEE department at the University of Liverpool. The authors would like to

gratefully acknowledge funding support from the University of Liverpool Doctoral Network in Technologies for Healthy Ageing. This work was partly funded by the UK National Biofilm Innovation Centre (grant numbers BB/R012415/1 and BB/X002950/1). The views expressed are those of the authors and not necessarily those of the University of Liverpool, the NIHR or the Department of Health and Social Care.

Author Contributions

The manuscript was written through contributions of all authors. All authors have given approval to the final version of the manuscript.

Data Availability Statement

The data that support the findings of this study are available from the corresponding author upon reasonable request.

Competing Interests

There are no conflicts to declare.

Figures

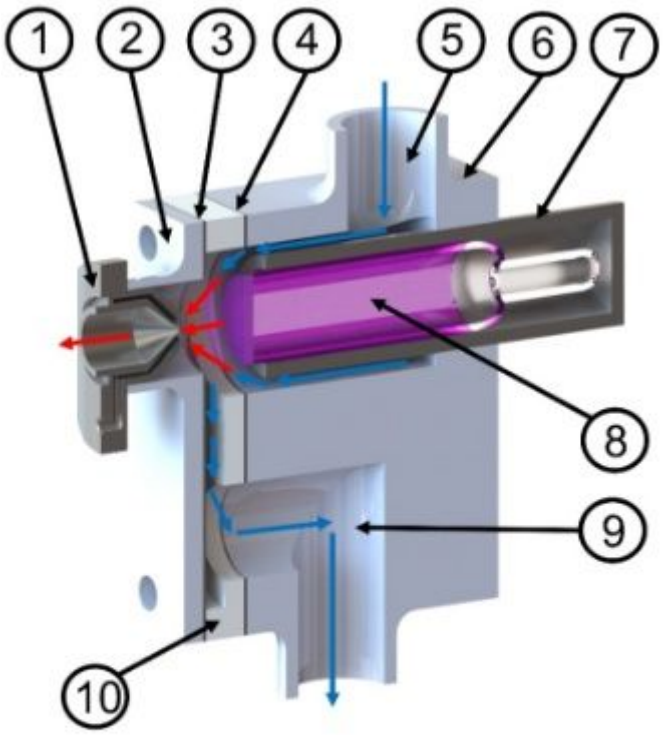

Figure 1

APPI sampling chamber; (1) MS inlet, (2) 3D printed end plate, (3) 2nd electrode, (4) 1st electrode, (5) sample entry, (6) 3D-printed body, (7) grounded metal collar for lamp, (8) UV lamp at 10.6eV, (9) exhaust, (10) PTFE electrode spacer. Blue arrows indicate the direction of sample gas flow. Red arrows indicate the direction of travel of photo generated ions.

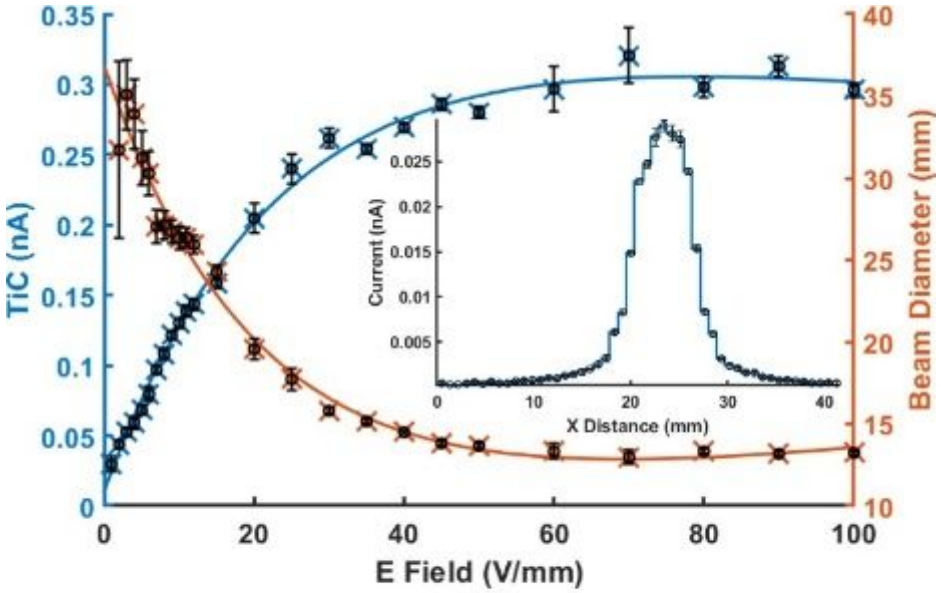

Figure 2

Total ion current (nA) and ion beam diameter (mm) measured by a segmented faraday detector for applied electric field between bias electrode and detector from 0 V/mm to 100 V/mm. Insert shows ion current hitting individual strips of the segmented detector when 5 V/mm field is applied.

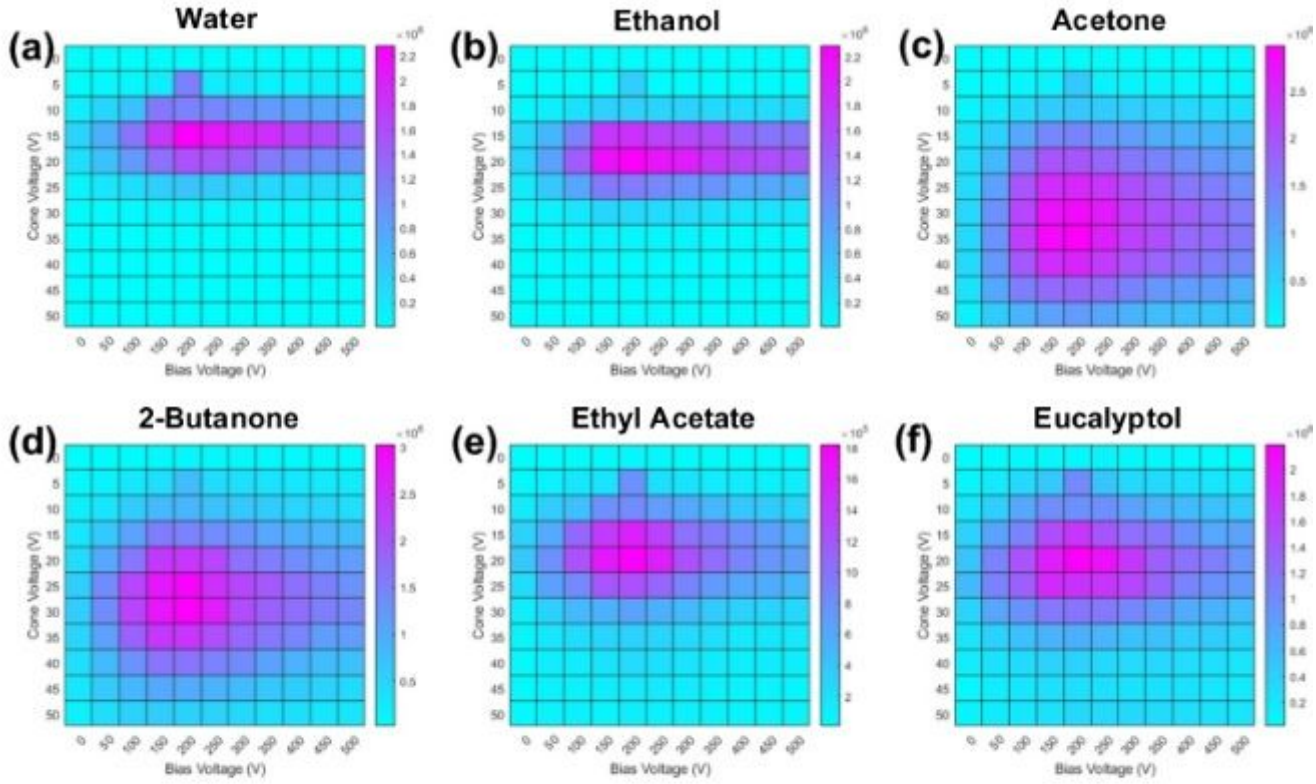

Figure 3

Optimisation heatmaps for (a) water, (b) ethanol, (c) acetone, (d) 2-butanone, (e) ethyl acetate and (f) eucalyptol, where light blue corresponds to low signal intensity and pink corresponds to high signal intensity, as per the scale bar included in each subfigure. The signal intensity is derived from each analyte's corresponding protonated molecular ion peak (see supporting information, Figure S2).

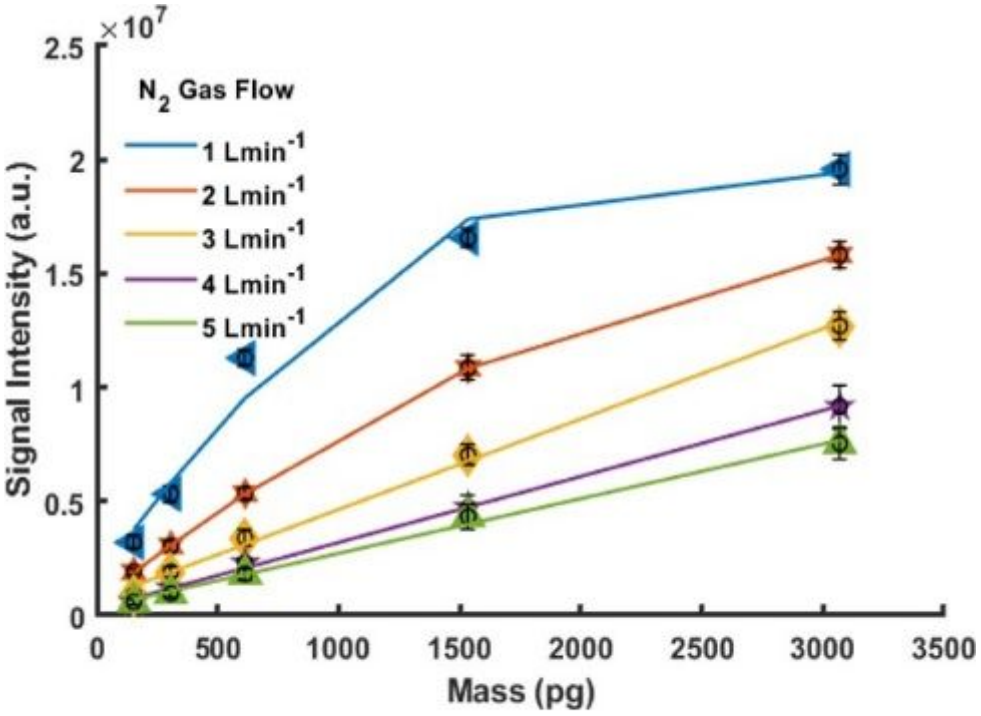

Figure 4

Signal intensity of eucalyptol (m/z 155) against the amount of analyte at a range of nitrogen gas flow rates from 1 to 5 $Lmin^{-1}$. Data are expressed as mean ± SD (n =3).

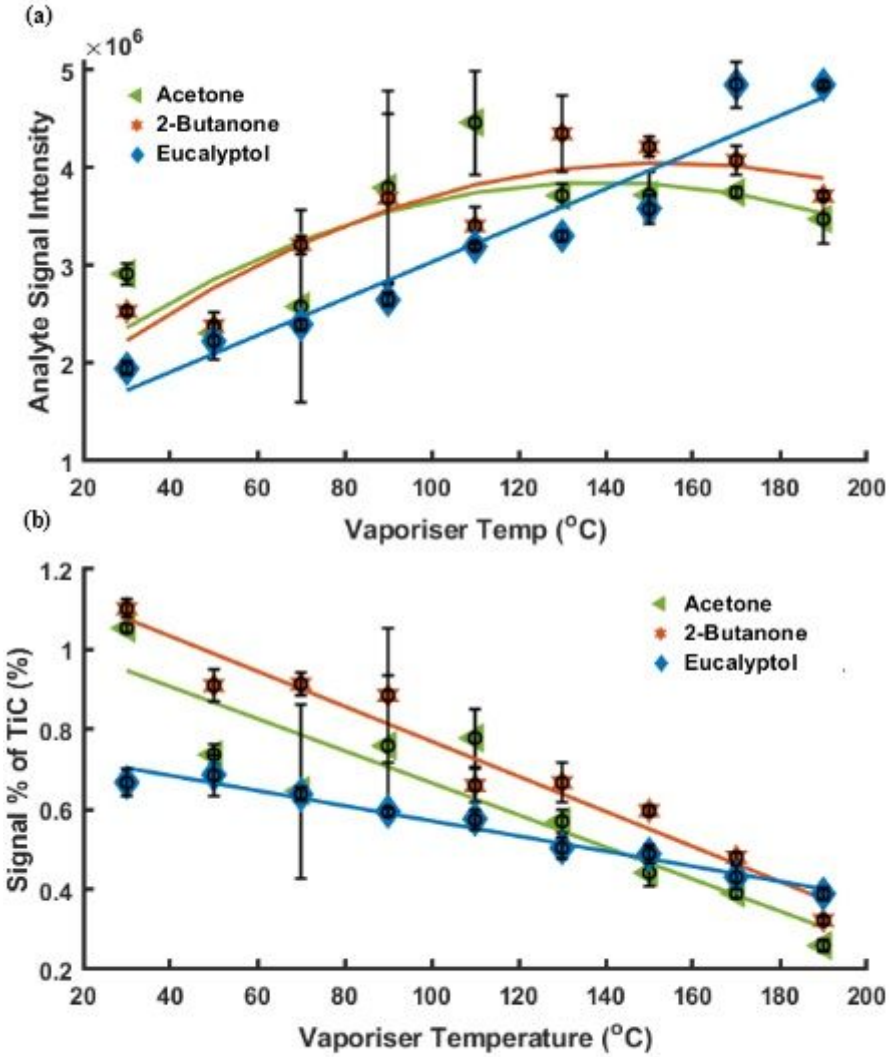

Figure 5

(a) Signal intensity of m/z 155 (Eucalyptol) for vaporisation temperature from 30 °C to 190 °C. (b) The peak height for m/z 155 is expressed as a percentage of the total ion current (TIC). Data are expressed as mean ± SD (n =3).

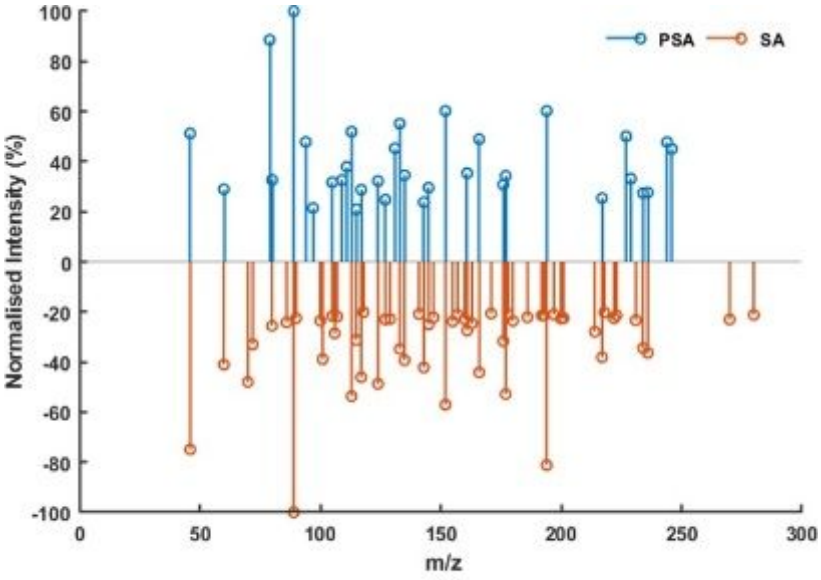

Figure 6

Centroided mass spectra showing all peaks with relative intensities > 20% for PSA and SA bacterial headspace samples.

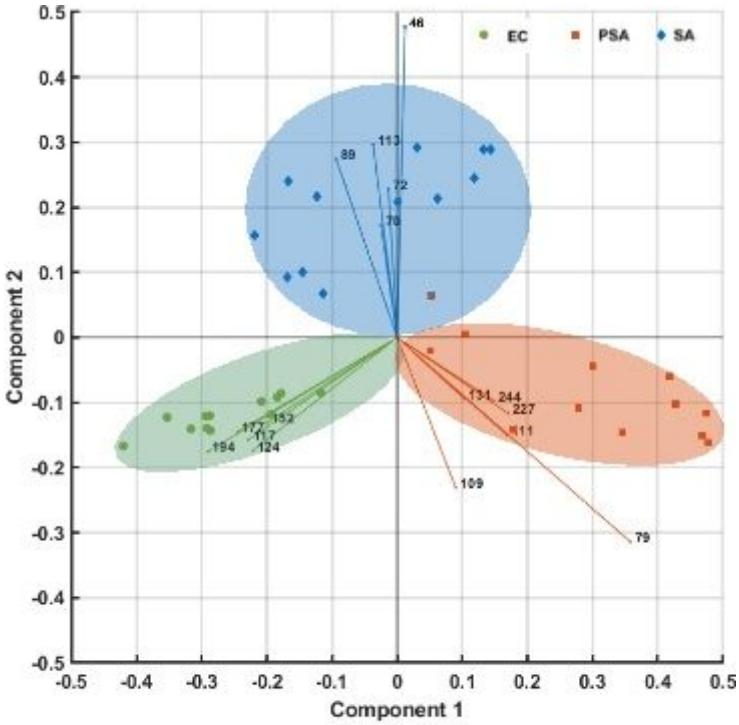

Figure 7

PCA biplot for 12 replicates of 3 types of bacterial culture samples (the numbers are the m/z ion peaks that contributed the most in each class for the classification model).

Supplementary Files

This is a list of supplementary files associated with this preprint. Click to download.

- FinalSI.pdf